

New constraints on the running-mass inflation model

Laura Covi¹, David H. Lyth² and Alessandro Melchiorri³

¹ *DESY Theory Group, Notkestrasse 85, D-22603 Hamburg, Germany.*

² *Physics Department, Lancaster University, Lancaster LA1 4YB, United Kingdom.*

³ *Astrophysics, Denys Wilkinson Building, University of Oxford, Keble road, OX1 3RH, Oxford, United Kingdom.*

(Dated: October 22, 2018)

We evaluate new observational constraints on the two-parameter scale-dependent spectral index predicted by the running-mass inflation model by combining the latest Cosmic Microwave Background (CMB) anisotropy measurements with the recent 2dFGRS data on the matter power spectrum, with Lyman α forest data and finally with theoretical constraints on the reionization redshift. We find that present data still allow significant scale-dependence of n , which occurs in a physically reasonable regime of parameter space.

I. INTRODUCTION.

The recent observation of the cosmic microwave background (CMB) angular anisotropies [1, 2, 3, 4, 5, 6, 7] have revealed an outstanding agreement between the data and the inflationary predictions of a flat universe and of a primordial scale invariant spectrum of adiabatic density perturbations (see e.g. [8, 9, 10, 11, 12, 13, 14, 15, 16]).

Furthermore, CMB measurements are in perfect agreement with other types of data and a global consistent picture is slowly emerging. For example, the CMB constraint on the amount of matter density in baryons, ω_b , is now consistent with the independent constraints from standard big bang nucleosynthesis (BBN) (see e.g. [17]). Also, the detection of power around the expected third peak, on arc-minutes scales, provides a new and independent evidence for the presence of non-baryonic dark matter (see e.g. [15]). At the same time, early data releases from the 2dFGRS and SDSS galaxy redshift surveys [18, 19] are living up to expectations and combined analysis of all these datasets are placing strong constraints on most of the cosmological parameters [15, 20, 21]. A combined analysis of both CMB and galaxy clustering is indeed necessary in order to break some of the degeneracies between the cosmological parameters that are affecting the single datasets. Recent combined analysis, for example, have provided important constraints on the amplitude of the matter fluctuations [15, 21], on the gravity waves background [20], on the dark energy equation of state [22, 23, 24] and on the neutrino mass [25, 26].

Thank to this new evidence, it is now accepted that the structure in the Universe is caused by an almost scale-independent primordial density perturbation, existing before cosmological scales start to enter the horizon. Nearly exponential inflation can easily explain the origin of this perturbation, because it converts the quantum fluctuation of every light scalar field into a scale-independent classical perturbation. At the present time, there is no equally successful alternative explanation for the origin of this perturba-

tion. In particular, there is no reason to expect the quantum-to-classical conversion to take place in extra space dimensions, though of course a string-theoretic description of such dimensions may play a vital indirect role by determining the form of the effective four-dimensional field theory.

In this paper, we combine the latest CMB and galaxy clustering data in order to place constraints on the inflationary model responsible for the primordial density perturbation. We will in fact assume the simple paradigm of a slowly-rolling inflaton field, whose perturbations are the seed for the primordial density perturbations [27, 28]¹. If this hypothesis is correct, observation will be able to distinguish between the few simple and well-motivated inflation models that exist, because they give different predictions for the spectral index of the primordial density perturbation. From among such models, we focus in this paper on the running-mass model of inflation [30, 31, 32, 33, 34, 35], which is the only one which can that can give a strongly scale-dependent (running) spectral index. Comparing with a suite of observations, we find that significant running is still allowed.

A similar attempt in constraining this kind of scale-dependence was made in [36] and [37], where however only a limited subset of the CMB and LSS data then available was used. A model-independent approach is used instead in [38], where constraints in the plane n and its first derivative $dn/d\ln k$ were obtained. The main difference with our approach is that there it is implicitly assumed that the scale dependence is small, while this is not necessary the case for the running mass model.

Our paper is organized as follows: In section II we discuss the running mass model. In section III we present our data analysis method and results. Finally, in section IV, we discuss our conclusions.

¹ The alternative [29] is to make a ‘curvaton’ field responsible, different from the inflaton if indeed the latter exists.

II. THE RUNNING MASS MODEL.

A. The potential

The running-mass model [30, 31, 32, 33, 34, 35] seems to be the only one which is both very well-motivated from the particle physics point of view and also presents a strong scale-dependence of the spectral index. The model is based on supersymmetry and identifies the inflaton field with a flat direction of the supersymmetric scalar potential. Global supersymmetry is broken during inflation by the large vacuum energy that drives inflation and so soft mass terms are generated for all scalar fields [39]. Taking the one-loop corrections to the tree-level potential into account, the most general expression for the potential along a flat direction, like the inflaton's, can then be cast into the form

$$V = V_0 + \frac{1}{2}m^2(\ln \phi)\phi^2 + \dots \quad (1)$$

where m^2 is the soft inflaton mass and the dots indicate non-renormalizable terms which are supposed to be negligible because ϕ/M_{P} is exponentially small (the usually-dominant renormalizable quartic term is absent precisely because we are using a flat direction in the scalar field space). The mass dependence on the renormalization scale, in our case identified with the value of the inflaton field, is given by the renormalization group equation [30]

$$\frac{dm^2}{d \ln \phi} \equiv \frac{dm^2}{d \ln Q} = \beta_m, \quad (2)$$

and therefore is proportional to the inflaton couplings, as given below in Eq. (3).

Ignoring for the moment the running, a generic supergravity theory will generate a soft mass-squared with magnitude at least of order $|m^2| \sim V_0/M_{\text{P}}^2$, which is marginally too big to support inflation. This is a problem for any model of inflation, whether or not the mass term is the one that is supposed to dominate. In all models except the running mass model, the problem is solved either by imposing a global symmetry to protect the flatness of the potential, or by supposing that the mass-squared is accidentally suppressed. The running mass model instead accepts the generic value of the mass-squared at the Planck scale (or some other high scale), and relies on the loop correction to sufficiently reduce it in the regime where inflation takes place.

For a particle with gauge and Yukawa interactions, we have that at one loop β_m is given by [31, 34]

$$\beta_m = -\frac{2C}{\pi}\alpha\tilde{m}^2 + \frac{D}{16\pi^2}|\lambda|^2 m_{\text{loop}}^2, \quad (3)$$

where the first term arises from gauge particles loops and the second from matter loops. Above C, D are a

positive group-theoretic numbers of order one, counting the degrees of freedom present in the loop, α is the gauge coupling, and \tilde{m} is the gaugino mass, while λ denotes a common Yukawa coupling and m_{loop}^2 the common susy breaking mass-squared of the scalar particles interacting with the inflaton via Yukawa interaction. Note that the first term in Eq. (3) is always negative, while the second has no definite sign, since m_{loop}^2 is defined as the mass squared splitting between scalar and fermionic superpartners and can have either sign. Also the case of a very-weakly-interacting inflaton gives $\beta_m \rightarrow 0$ and so that the constant mass potential is recovered.

Over a sufficiently small range of ϕ , or for very small inflaton couplings, it is a good approximation to take a Taylor expansion of the running mass $m^2(\ln \phi)$ and then we have:

$$V = V_0 + \frac{1}{2}m^2(\ln \bar{\phi})\phi^2 - \frac{1}{2}c(\ln \bar{\phi})\frac{V_0}{M_{\text{P}}^2}\phi^2 \ln(\phi/\bar{\phi}), \quad (4)$$

where we have expanded around $\bar{\phi}$, and rescaled the last term w.r.t. V_0/M_{P}^2 for future convenience. The dimensionless constant c is proportional to the mass beta function,

$$c = -M_{\text{P}}^2\beta_m/V_0 \quad (5)$$

It has been shown [33] that for small c , as is required by slow roll conditions, the linear approximation is very good over the range of ϕ corresponding to horizon exit for scales between k_{COBE} and $8h^{-1}$ Mpc. In order to obtain also a crude estimation of the reionization epoch via the Press-Schechter formula, which involves the power spectrum at a scale of order $k_{\text{reion}}^{-1} \sim 10^{-2}$ Mpc (enclosing the relevant mass of order $10^6 M_{\odot}$), we shall assume that the linear approximation is adequate down to this 'reionization scale'.

For studying the inflaton potential, it is very useful to introduce a new parameter ϕ_* via

$$m^2(\bar{\phi}) = \frac{V_0}{M_{\text{P}}^2} c(\bar{\phi}) \left[\ln \left(\frac{\phi_*}{\bar{\phi}} \right) + \frac{1}{2} \right]. \quad (6)$$

Then Eq. (7) takes the simple form [33]

$$V = V_0 - \frac{1}{2} \frac{V_0}{M_{\text{P}}^2} c\phi^2 \left(\ln \frac{\phi}{\phi_*} - \frac{1}{2} \right), \quad (7)$$

leading to

$$\frac{V'}{V_0} = -c \frac{\phi}{M_{\text{P}}^2} \ln \frac{\phi}{\phi_*}, \quad (8)$$

In typical cases the linear approximation is valid at $\phi = \phi_*$, and that point is then a maximum or a minimum of the potential.

The running-mass model supposes that the relevant soft masses at the Planck scale (or some other high scale) have magnitude roughly of order

$$|\text{soft mass}| \sim V_0^{\frac{1}{2}}/M_{\text{P}} \sim H, \quad (9)$$

and that the relevant couplings (gauge or Yukawa) are very roughly of order 1. In general, one of the loops will dominate over the others making only one soft mass relevant besides the inflaton mass. With these assumptions, the coupling c defined by Eq. (5) is roughly

$$|c| \sim 10^{-1} \text{ to } 10^{-2}. \quad (10)$$

A bigger value of $|c|$ is unviable because it would not allow inflation. On the other hand, using Eq. (7) as a very crude estimate of the inflaton mass at the Planck scale, one can see that a much smaller value of $|c|$ is probably not viable either, since it would require the inflaton mass at that scale to be suppressed below the estimate Eq. (9).

For scalar masses, the estimate Eq. (9) is expected to be valid provided that the following statements are true: (i) there is at most gravitational-strength coupling between the inflaton sector and the sector in which SUSY is spontaneously broken (ii) this breaking comes from an F term as opposed to a D term (iii) during inflation (in contrast to the situation in the vacuum) the F term in the potential is *not* accurately canceled by the other, negative contribution to the potential. The third of these requirements is reasonable provided that the potential satisfies

$$V_0 \gtrsim M_S^4, \quad (11)$$

where M_S is the SUSY-breaking scale in the vacuum.

The most economical assumption is that actually the mechanism of spontaneous SUSY breaking during inflation is basically the same as it is in the vacuum, making V_0 roughly of order M_S^4 . For respectively the cases of anomaly-mediated, gravity-mediated and (low-energy) gauge-mediated transmission of SUSY-breaking to the Standard Model sector, this leads to the rough estimates

$$V_0^{\frac{1}{4}} \sim 10^{12} \text{ GeV} \quad (12)$$

$$V_0^{\frac{1}{4}} \sim 10^{10} \text{ GeV} \quad (13)$$

$$V_0^{\frac{1}{4}} \sim 10^6 \text{ GeV}. \quad (14)$$

The second case was assumed in the original works [30, 31, 39]. It gives the correct normalization for the spectrum for reasonable parameters, but there is probably enough latitude to allow the first or even the third case.

We emphasize that the estimate Eq. (9) for the scalar soft masses in the inflaton sector is reasonable in all three cases, even though the soft masses in the Standard Model sector (evaluated of course in the vacuum, and of order 100 GeV) satisfy that estimate only in the second, gravity-mediated case. In the first (anomaly-mediated) case, this is because no-scale supergravity does not automatically suppress soft scalar masses during inflation, as it does in the vacuum [27]. In the third (gauge-mediated) case it is because one

can easily suppose that the gauge-mediation mechanism simply does not operate in the inflaton sector. If the relevant soft mass is a gaugino mass, the expectation of Eq. (9) is not so automatic because gaugino masses can be very small with some types of SUSY breaking, but it is not unreasonable either.

In summary, we expect c in the range (10) in a typical running mass model of inflation. As we now see, this typically leads to significant scale-dependence of the spectral index.

B. The spectrum and the spectral index

Now we come to the predicted spectrum and spectral index of the primordial density perturbation. We suppose that it is generated by the inflaton field perturbation, which means that it is purely adiabatic and gaussian. It is therefore specified by the curvature perturbation $\mathcal{R}(k)$, with k as usual the comoving wavenumber. This quantity is gaussian and hence specified by its spectrum $\mathcal{P}_{\mathcal{R}}(k)$.

To give the prediction of the running mass model for the spectrum, it is convenient to define

$$s \equiv c \ln(\phi_*/\phi_{\text{COBE}}), \quad (15)$$

where the subscript COBE denotes the epoch of horizon exit for the COBE scale $k_{\text{COBE}} \simeq 0.002(h/\text{Mpc})$.

Instead of the spectrum $\mathcal{P}_{\mathcal{R}}(k)$ we work with the conventional quantity $\delta_H \equiv \frac{2}{5}\mathcal{P}_{\mathcal{R}}^{1/2}$. At the COBE scale, the prediction of the running-mass model is

$$\delta_H(k_{\text{COBE}}) = \frac{1}{5\pi\sqrt{3}} \frac{V_0^{\frac{1}{2}}}{M_{\text{P}}\phi_*} |s|^{-1} \exp(s/c). \quad (16)$$

As already mentioned, the observed value $\delta_H(k_{\text{COBE}}) = 1.9 \times 10^{-5}$ is easily obtained, for choices of V_0 and ϕ_* that correspond to reasonable particle physics assumptions.

In this paper we concern ourselves with the dramatic scale-dependence of the spectrum, which is given by

$$\frac{\delta_H^2(k)}{\delta_H^2(k_{\text{COBE}})} = \exp \left[\frac{2s}{c} \left(e^{c\Delta N(k)} - 1 \right) - 2c\Delta N(k) \right], \quad (17)$$

where $\Delta N(k) \equiv N_{\text{COBE}} - N(k) \equiv \ln(k/k_{\text{COBE}})$. We plot the primordial power spectrum for the running mass model in comparison to the constant spectral index case in Figure 1.

To discuss the spectral index and its running, we need the first four derivatives of the potential,

$$M_{\text{P}}^2 \frac{V'}{V_0} = -c\phi \ln \frac{\phi}{\phi_*} \quad (18)$$

$$M_{\text{P}}^2 \frac{V''}{V_0} = -c \left(\ln \frac{\phi}{\phi_*} + 1 \right) \quad (19)$$

$$M_{\text{P}}^2 \frac{V'''}{V_0} = -\frac{c}{\phi} \quad (20)$$

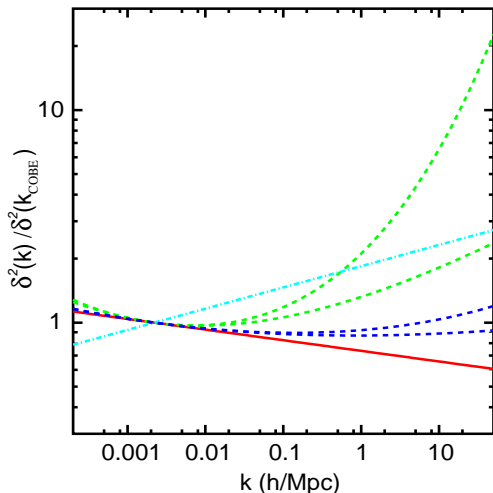


FIG. 1: Primordial power spectrum on a logarithmic plot for the case of a scale invariant spectral index $n = 0.95$ (solid line) and $n = 1.1$ (dashed-dotted line), and for the running mass prediction with $n_{\text{COBE}} = 0.95$ and two different n'_{COBE} , i.e. $n'_{\text{COBE}} = 0.04$, corresponding to $c = 0.1545$, $s = 0.1295$ (upper dashed line) or $c = -0.1545$, $s = -0.1295$ (lower dashed line), and $n'_{\text{COBE}} = 0.01$, corresponding to $c = 0.08431$, $s = 0.05931$ (upper dotted line) or $c = -0.05931$, $s = -0.08431$ (lower dotted line).

$$M_{\text{P}}^2 \frac{V''''}{V_0} = \frac{c}{\phi^2} \quad (21)$$

Introducing s , the first four flatness parameters [27, 28] are (setting $V = V_0$ in the denominators)

$$\epsilon \equiv \frac{1}{2} \left(\frac{M_{\text{P}}^2 V''}{V} \right)^2 \simeq \frac{s^2 \phi^2}{M_{\text{P}}^2} e^{c\Delta N(k)} \quad (22)$$

$$\eta \equiv \frac{M_{\text{P}}^2 V'''}{V} \simeq s e^{c\Delta N(k)} - c \quad (23)$$

$$\xi^2 \equiv \frac{M_{\text{P}}^4 V' V''''}{V} \simeq -c s e^{c\Delta N(k)} \quad (24)$$

$$\sigma^3 \equiv \frac{M_{\text{P}}^6 V'^2 V''''}{V} \simeq c s^2 e^{2c\Delta N(k)}. \quad (25)$$

The parameters are evaluated at the epoch of horizon exit for the scale k . The first parameter ϵ is negligible because ϕ/M_{P} is taken to be exponentially small. The condition for slow-roll inflation is therefore just $|\eta| \ll 1$, which is satisfied in the regime $\phi \sim \phi_*$ provided that $|c| \ll 1$. This corresponds also to requiring $|s| \ll 1$.

Additional and generally stronger constraints on s follow from the reasonable assumptions that the mass continues to run to the end of slow-roll inflation, and that the linear approximation remains *roughly* valid. Discounting the possibility that the end of inflation is very fine-tuned, to occur close to the maximum or minimum of the potential, we have the lower bound

$$|s| \gtrsim e^{-cN_{\text{COBE}}} |c|. \quad (26)$$

Note that for negative c , this constraint is very strong, requiring a very large value of s even for small c and a

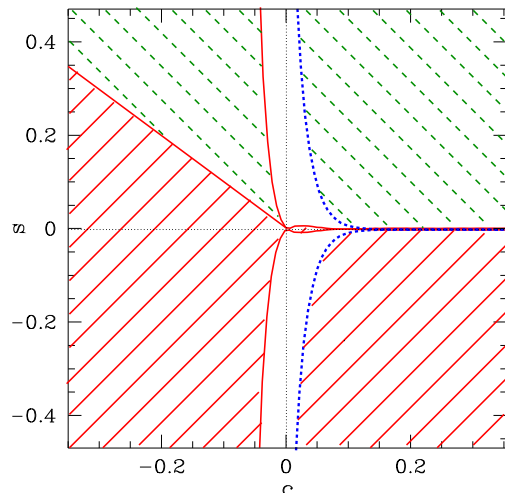


FIG. 2: Theoretical expected value of the parameters c, s for $N_{\text{COBE}} = 50$; the solid-line-hatched region is strongly excluded by naturality assumptions, while the dashed-line-hatched region is only weakly excluded. The dotted line shows the prediction for the simplest case, $s = e^{-cN_{\text{COBE}}}$, where the linear approximation is valid up to the end of inflation, triggered by $\eta = 1$.

kind of fine-tuning between s and c to give a reasonable value of $n - 1$.

For positive c , we also obtain a significant upper bound by setting $\Delta N = N_{\text{COBE}}$ in Eq. (30), and remembering that slow-roll requires $|n - 1| \lesssim 1$:

$$|s| \lesssim e^{-cN_{\text{COBE}}} \quad (c > 0). \quad (27)$$

In the simplest case, that slow-roll inflation ends when $n - 1$ actually becomes of order 1, this bound becomes an actual estimate, $|s| \sim e^{-cN_{\text{COBE}}}$. As discussed in [36], this upper bound can be relaxed for positive s if the running of the mass ceases before the end of slow-roll inflation. The approximate region of the s versus c plane excluded by these considerations is shown in Figure 2.

Since ϵ is negligible, the spectral index is

$$n(k) = 1 + 2\eta - 6\epsilon \quad (28)$$

$$\simeq 1 + 2\eta. \quad (29)$$

This gives [36]

$$\frac{n(k) - 1}{2} = s e^{c\Delta N(k)} - c. \quad (30)$$

The first derivative of the spectral index is given by

$$n'(k) \equiv \frac{dn(k)}{d \ln k} = 2sc e^{c\Delta N(k)}. \quad (31)$$

Clearly the spectral index is not constant within cosmological unless s or c is very close to zero.

At the COBE scale,

$$n_{\text{COBE}} - 1 = 2(s - c) \quad (32)$$

$$n'_{\text{COBE}} = 2sc. \quad (33)$$

The straight line $s = c$ in the s vs c plane corresponds to $n_{\text{COBE}} = 1$. The scale independent case of constant $n = 1$ is given by the origin $s = c = 0$, while constant spectral index different from 1 is realized either on the $c = 0$ axis for $s = (n - 1)/2$ or on the $s = 0$ axis for $c = -(n - 1)/2$.

Taking cosmological scales to span a range $\Delta N \sim 10$, we see that the running mass model generates a change $\delta n \sim 10sc$ in the spectral index. This change should eventually be detectable unless both $|c|$ and $|s|$ are towards the bottom of their expected ranges.

We will show in the following the allowed region both in the s, c parameter space and in the n'_{COBE} vs $n_{\text{COBE}} - 1$ plane. Note in this respect that not all values of n'_{COBE} are allowed in the running mass models: from the definition above, we obtain the constraint

$$n'_{\text{COBE}} \geq -\frac{(n_{\text{COBE}} - 1)^2}{4}, \quad (34)$$

so that a decreasing spectral index is possible only if n_{COBE} is different from 1. Also Eq. (33) is symmetric under reflection with respect to the $s + c = 0$ line, so fixing the variables $n_{\text{COBE}} - 1$ and n'_{COBE} determines two values of s, c . We will investigate in the following how strongly the data are sensitive to a variation of n' and therefore able to disentangle this degeneracy. From all this, it follows that fitting for arbitrary value of n' is not exactly equivalent to performing a fit for the running mass models.

These predictions for the spectral index and its derivative are to leading order in slow-roll. To second order, the spectral index is given to a good approximation by [27]

$$\frac{n(k) - 1}{2} = s(1 + 1.06c)e^{c\Delta N(k)} - c, \quad (35)$$

We neglected a term of order η^2 , and the remaining (unknown) error is expected to be of order σ^3 . Both of these are negligible which means that the second-order correction should be rather accurate. We shall not include it though, because it just corresponds to a small rescaling of the quantity s , whose precise value depends on unknown physics [27]. Note that it is in any case easy to obtain the results at next-to-leading order, by rescaling s by the factor $1/(1 + 1.06c)$ or shift $n_{\text{COBE}} - 1$ by $1.06 n'_{\text{COBE}}$.

III. OBSERVATIONAL CONSTRAINTS

A. Method

We compare the recent cosmological observations with a grid of theoretical models computed with the public available CMBFAST [40] code. We restrict our analysis to flat, adiabatic, Λ -CDM models and we sample the various parameters as follows:

$\Omega_{\text{cdm}}h^2 \equiv \omega_{\text{cdm}} = 0.01, \dots, 0.40$, in steps of 0.01; $\Omega_b h^2 \equiv \omega_b = 0.001, \dots, 0.040$, in steps of 0.001 and $\Omega_\Lambda = 0.0, \dots, 0.95$, in steps of 0.05. The value of the Hubble constant is given by $h = \sqrt{\frac{\omega_{\text{cdm}} + \omega_b}{1 - \Omega_\Lambda}}$.

We allow for a reionization of the intergalactic medium by varying also the compton optical depth parameter τ_c in the range $\tau_c = 0.0, \dots, 0.20$ in steps of 0.05. Greater values of τ_c are in disagreement with recent estimates of the redshift of reionization $z_R \sim 6 \pm 1$ (see e.g. [41]) which points towards $\tau_c \sim 0.05$. As discussed later, given a cosmological model, we checked for the consistency of the assumed optical depth with its expected values derived from a simple reionization scenario.

We vary the 2 parameters of the running mass model in the range $-0.30 < c < 0.30$ and $-0.47 < s < 0.47$ in a 50×50 grid. To save computing time, we compute the CMB anisotropies transfer functions for each cosmological model just one time and then we integrate them different times looping over c and s .

For the CMB data, we use the recent results from the BOOMERanG-98, DASI, MAXIMA-1, CBI, and VSA experiments. The power spectra from these experiments were estimated in 19, 9, 13, 14 and 10 bins respectively (for the CBI, we use the data from the MOSAIC configuration), spanning the range $2 \leq \ell \leq 3500$. However, since in this work we are interested only in comparing the data with the expected *primary* anisotropies, we limit our analysis to the region $\ell < 1500$ which is likely not to be affected by secondary effects like Sunyaev-Zel'dovich (see e.g. [42]).

The likelihood for a given theoretical model is defined by $-2\ln\mathcal{L} = (C_B^{\text{th}} - C_B^{\text{ex}})M_{BB'}(C_{B'}^{\text{th}} - C_{B'}^{\text{ex}})$ where $M_{BB'}$ is the Gaussian curvature of the likelihood matrix at the peak and C_B are the experimental (theoretical) band powers. We discard the first bin of the CBI dataset ($0 < \ell < 400$), due to the asymmetric window function and the high sample variance.

We consider 10%, 4%, 5%, 3.5% and 5% Gaussian distributed calibration errors for the BOOMERanG-98, DASI, MAXIMA-1, VSA, and CBI experiments respectively and we include the beam uncertainties by the analytical marginalization method presented in [43].

In addition to the CMB data we incorporate the real-space power spectrum of galaxies in the 2dF 100k galaxy redshift survey using the data and window functions of the analysis of Tegmark et al. [44].

To compute \mathcal{L}^{2dF} , we evaluate $p_i = P(k_i)$, where $P(k)$ is the theoretical matter power spectrum and k_i are the 49 k-values of the measurements in [44]. Therefore we have $-2\ln\mathcal{L}^{2dF} = \sum_i [P_i - (Wp)_i]^2 / dP_i^2$, where P_i and dP_i are the measurements and corresponding error bars and W is the reported 27×49 window matrix. We restrict the analysis to a range of scales where the fluctuations are assumed to be in the linear regime ($k < 0.2h^{-1}\text{Mpc}$). When combin-

ing with the CMB data, we marginalize over a bias b considered to be an additional free parameter.

We also include the recent 13 data points on the matter power spectrum obtained by Croft et al. [45] using Lyman α forest data from 53 quasar spectra. The theoretical transfer functions are in this case computed up to redshift $z = 2.72$ and compared by a simple chi-square analysis with the data, including the $\pm 25\%$ error in the data amplitude.

Moreover, following a similar approach used in a previous analysis [37] we use reionization bounds. Practically, we deduce for each theoretical model, the expected value of τ_c^{th} ,

$$\tau_c^{th} = \frac{0.035 \Omega_b h}{1 - \Omega_\Lambda} \left(\sqrt{(1 - \Omega_\Lambda)(1 + z_R)^3 + \Omega_\Lambda} - 1 \right) \quad (36)$$

from the reionization redshift z_R estimated using a Press-Schechter formula. Taking f to be the fraction of matter collapsed into objects with mass $M = 10^6 M_\odot$, $1 + z_R$ is given by

$$1 + z_R \simeq \begin{cases} \frac{\sqrt{2}\sigma(M)}{\delta_c g(1 - \Omega_\Lambda)} \operatorname{erfc}^{-1}(f) & f \ll 1 \\ \frac{\sigma(M)}{g(1 - \Omega_\Lambda)} & f \simeq 1 \end{cases} \quad (37)$$

where $\sigma(M)$ is the present, linearly evolved, rms density contrast with top-hat smoothing and $\delta_c = 1.7$ is the overdensity contrast required for gravitational collapse; $g(1 - \Omega_\Lambda)$ is the suppression factor of $\sigma(M)$ at the present epoch for the case of a non vanishing cosmological constant:

$$g(\Omega) = \frac{5}{2} \Omega \left(\frac{1}{70} + \frac{209}{140} \Omega - \frac{1}{140} \Omega^2 + \Omega^{4/7} \right)^{-1}. \quad (38)$$

In the case of the running mass model, $\sigma(M)$ can become very large even for moderate values of c , if $c \ln(k_R/k_{COBE}) \simeq 1$, so that the reionization constraint is very powerful. To give a feeling of this strong dependence, we show in Figure 3 the value of z_R as a function of c for the simple cases $s = c, s = c - 0.05$ at fixed cosmological parameters.

For each model in the database with a given optical depth τ_c we then consider the further prior $2 \ln \mathcal{L}^{rei} = [\tau_c - \tau_c^{th}]^2 / 0.05^2$ where the $1 - \sigma$ error should take into account the uncertainties due to the different reionization mechanisms.

Finally, we also include a constraint on the variance σ on a mass scale of $10^6 h^{-1} M_\odot$ of 9 ± 1 consistent with the limits on the linear power spectrum obtained using measurements of substructure in gravitational lens galaxies in the analysis of [46].

One should keep in mind that there are many caveats in the inclusion of all above constraints.

We attribute a likelihood to each value of c and s by marginalizing over the *nuisance* parameters. We then define our 68% (95%), confidence levels to be where the integral of the likelihood is 0.16 (0.025) and 0.84 (0.975) of the total value.

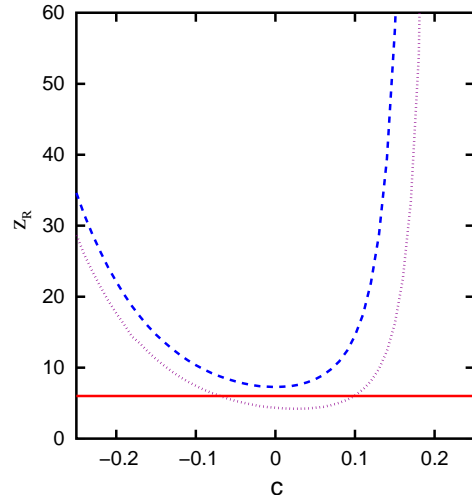


FIG. 3: Theoretical expected value of z_R for $f \simeq 1$ as a function of c for the case $s = c$ (dashed curve) and $s = c - 0.05$ (dot-dashed curve). The cosmological parameters are chosen as $h = 0.72$, $\omega_{cdm} = 0.086$ and $\omega_b = 0.02$. We show also the reference line $z_R = 6$ (solid line).

B. Results

The likelihood contours in the $c - s$ plane obtained analyzing the CMB data under the assumption of a set of “weak” priors ($h = 0.65 \pm 0.2$, $t_0 > 11 Gyr$) are plotted in Figure 4. As we can see, even if the space of models analyzed is quite broad, the CMB data is able to give strong constraints along the $s - c$ direction. In particular, we obtain the constraint $n_{COBE} = 1 + 2(s - c) = 0.96_{-0.04}^{+0.06}$ and n_8 is at 68% c.l.. We found that including stronger priors ($h = 0.72 \pm 0.08$, $\Omega_m = 0.3 \pm 0.1$) on the nuisance parameters does not change these results and does not improve significantly the constraints on n_{COBE} . Assuming negligible reionization ($\tau = 0$) gives $n_{COBE} = 0.93_{-0.03}^{+0.03}$.

Also plotted in Figure 4 (Top Panel) are the likelihood contours obtained in the combined 2dFGRS-CMB analysis. As we can see, even the inclusion of the 2dF data does not improve significantly the CMB constraints. The combination of the 2dF data is extremely powerful in constraining parameters like Ω_m and h , that define the epoch of equality and the position in the k space of the matter spectrum. However, in the CMB+2dF combined analysis, we found $n_{COBE} = 0.97_{-0.04}^{+0.05}$ at 68% c.l..

In the center panel of Figure 4 we report the likelihood contours obtained in the combined CMB+Ly- α analysis. As already noticed by [38], we find that the Lyman α data are able to restrict more strongly the scale dependence of the spectral index and therefore exclude the parameter space at large $|c|$; in particular at 68% we have $sc < 0.026$, so that a variation of the spectral index over cosmological scale of the order of 10% is allowed.

Finally, in the bottom panel of Figure 4 we plot

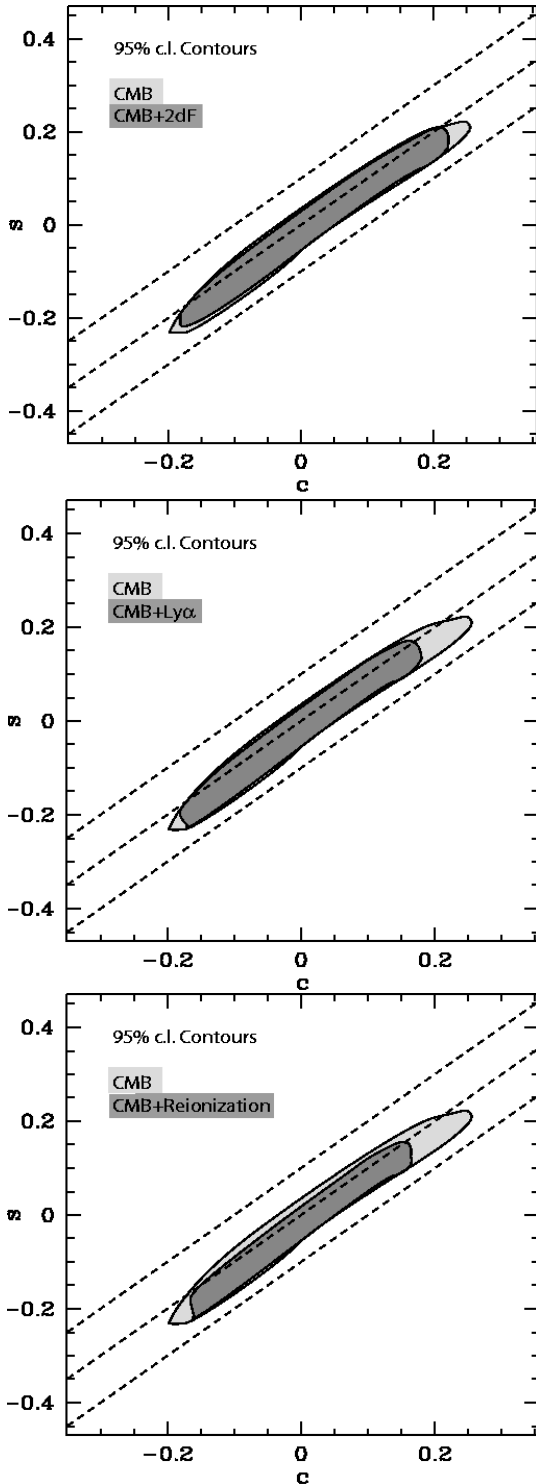


FIG. 4: Likelihood contours in the $c - s$ plane. The gray contours are the 95% c.l. from the CMB analysis. The dark contours are from CMB+2dF analysis (Top), CMB+Ly α (Center Panel), CMB+Reionization constraint (Bottom Panel). The straight lines corresponds to $n_{\text{COBE}} = 0.8, 1.0$ and 1.2 .

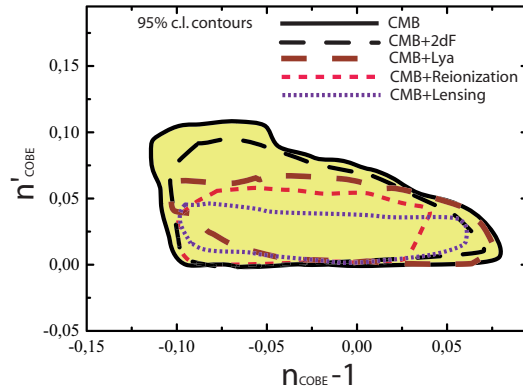


FIG. 5: Likelihood contours in the $(n_{\text{COBE}} - 1) - (n'_{\text{COBE}})$ plane for different datasets.

the likelihood contours obtained in the combined CMB+reionization analysis. Also in this case part of the region of large s, c is excluded, but still a sizable variation and values of $|c|$ up to 0.2 are allowed. It should be emphasized that this reionization constraint is only one of theoretical consistency. As one can see from Figure 3, the self-consistent value of z_R becomes very large for $c > 0.10$. If it turns out that $z_R \lesssim 10$, the top part of the allowed region ‘CMB + Reionization’ will be excluded.

Focussing on the region ($s + c > 0$, $c > 0$), we plot the likelihood contours in the $2(s - c)$ vs. $2sc$ plane in Figure 5. As we explained before, $2(s - c)$ gives the value of the spectral index $n_{\text{COBE}} - 1$ on COBE scales, while $2sc = n'_{\text{COBE}}$ gives the bend in the spectrum.

As we can see from the figure, the recent CMB data alone constrains $n'_{\text{COBE}} < 0.1$ at 95% C.L., while including the constraints from 2dF, Ly- α , reionization redshift, limits the amount of deviation from scale invariance to $n'_{\text{COBE}} < 0.05$ at 95% c.l.. Adding the strong lensing constraint from [46], as discussed earlier, further constrains $n' < 0.04$ at 95% c.l.. It is important to notice that a lower spectral index $n < 0.95$ is consistent with the lensing observation only if $n'_{\text{COBE}} > 0$. Note also that in all cases the best fit value of n'_{COBE} is not in the centre of the allowed region, but lower, towards the value $n'_{\text{COBE}} = 0$. Furthermore, the inclusion of a bend in the power spectrum, does not seem to affect in a considerable way the CMB constraint on n since there is a weak correlation between these two variables.

The correlation between n'_{COBE} and the remaining parameters is investigated in Figure 6 where the likelihood function for n'_{COBE} is plotted in function of ω_b , ω_{cdm} and the Hubble parameter, h .

As we can see, the correlation with these parameters is extremely small, meaning that the inclusion of a bending in the primordial spectrum would not drastically affect the actual constraints on the parameters considered. However, an increase in n'_{COBE} can al-

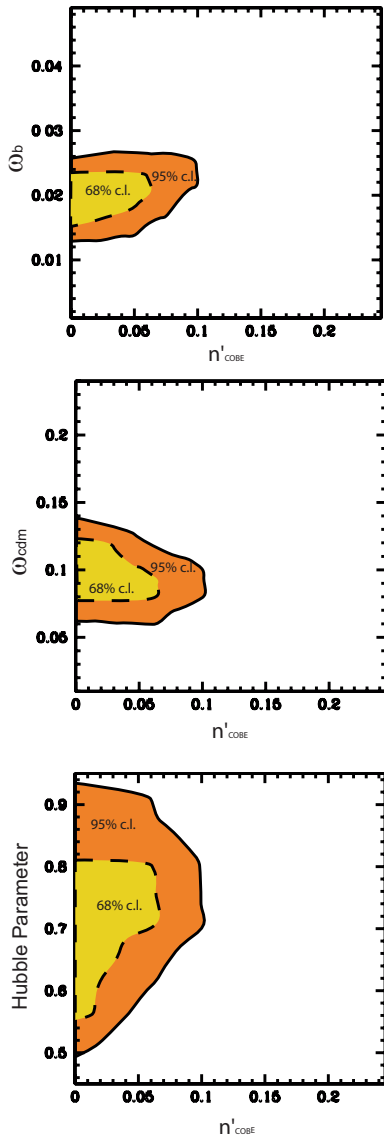


FIG. 6: Correlations between n'_{COBE} with different parameters. From top to bottom, we consider the physical density in baryons ω_b , in cold dark matter ω_{cdm} and the Hubble parameter, h .

low larger (smaller) values of ω_b (ω_{cdm}). The Hubble parameter h is poorly constrained by CMB alone.

We have also considered the effect of variations in n_{COBE} and n'_{COBE} on the predicted level of rms mass fluctuations in spheres of $8h^{-1}$ Mpc. At the moment, there is some sort of tension between the possible values of this parameter obtained from local cluster abundances ($\sigma_8 \sim 0.75$ for $\Omega_M = 0.3$, see e.g. [47]) and weak lensing ($\sigma_8 \sim 0.9$ for $\Omega_M = 0.3$ see e.g. [48]).

In Figure 7 we plot the likelihood contours from the CMB analysis for σ_8 against $n_{\text{COBE}} - 1$ (Top Panel) and n'_{COBE} (Bottom Panel) respectively. As expected, increasing both $n_{\text{COBE}} - 1$ and n'_{COBE} increases the level of σ_8 , but the correlation is not relevant enough to actually detect a bending in the spectrum with

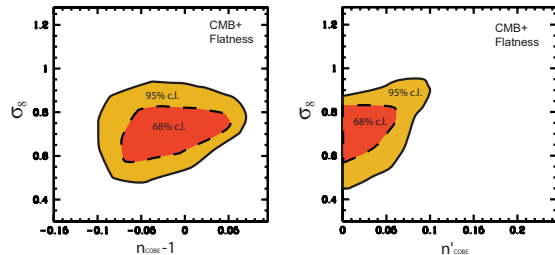


FIG. 7: Likelihood contours in the $(n_{\text{COBE}} - 1) - \sigma_8$ (Top) and $n'_{\text{COBE}} - \sigma_8$ planes.

present observations.

We are in qualitative agreement with other recent constraints on a running spectral index [38]. Precise comparison is difficult mainly because we did not consider a background of gravity waves (that can weaken our final result) since in the running-mass models this is negligible. Furthermore, we considered a more updated CMB dataset respect to the one considered in [38] and we considered different datasets other than CMB. Finally, [38] assumes that n' can take any value, whereas the running-mass model excludes significantly negative n' (Eq. (34)). The running-mass model also allows variation of $n'(k)$, but this is not very significant at the present level of observation.

We end this discussion of our results by commenting on a recent analysis by Caprini, Hansen and Kunz [49] which investigates the variation of $n'(k)$ that is allowed by observation. First, they assume that the flatness parameter σ^3 is constant to the end of slow-roll inflation, and taking $N_{\text{COBE}} = 50$, they find $\sigma^3 > -3.5 \times 10^{-4}$. The running-mass prediction Eq. (25) for σ^3 is roughly constant to the end of slow-roll inflation if $|c| \lesssim 1/50$, and in this regime one needs $|s| \lesssim 0.1$ to have n sufficiently close to 1; combining these results gives roughly $|\sigma^3| \lesssim 4 \times 10^{-4}$ in agreement with [49]. However, [49] assume next that instead V'''' is roughly constant, and derives a bound $M_{\text{P}}^4 V''''/V > -0.02$. In contrast, the running-mass model predicts $M_{\text{P}}^4 V''''/V = c(M_{\text{P}}/\phi)^2$ which is exponentially large (and of either sign) and strongly varying. Thus the bound on V'''' of [49] does not apply to the running-mass model in any regime of its parameter space. We remind the reader again that, at the moment, the running-mass model is the only well-motivated model giving significant running of the spectral index.

IV. CONCLUSIONS

The rather full analysis that we have described confirms the general picture indicated by previous analyses [37]. The allowed region in the c vs s plane depicted in Figure 4 should be compared with the region shown in Figure 2 which approximately delin-

eates the theoretically disfavoured region, and also with the minimum value $|c| \gtrsim 10^{-2}$ which is probably needed to generate enough running of the mass even if we go from the Planck scale to 100 GeV. Combining all of these, we see that if $|c|$ is significantly above the minimum value, only the version of the model with c and s both positive is viable. In that case, the spectral index has significant running which will be detectable in the foreseeable future. On the other hand, if $|c|$ is really of order 10^{-2} , all choices of the signs of c and s are possible except maybe negative c with positive s . Furthermore, if that extreme case can be realized in a viable running-mass model the running of n will be so small that it may never be detectable.

Looking at the observational situation in more detail, our results show that the CMB data can put very strong constraints on the value of the spectral index at large scales, $n_{COBE} = 1 + 2(s - c)$, but still allow a pretty large scale-dependence. Other information on

the power spectrum, like Lyman α data, or strongest assumptions about the reionization epoch are needed to reduce the parameter space in the $s + c$ direction. Still values of $|c|$ of the order of 0.2, and therefore n'_{COBE} of the order 0.04, are allowed. Note also that our allowed region is more or less symmetric under reflection with respect to the $s + c = 0$ line: this means that the present data are not sensitive enough to distinguish the variation of n' that is predicted by the running-mass model. Finally, we show that the inclusion of the running in the spectral index has a moderate effect on the present CMB determination of the physical matter densities in baryons ω_b and cold dark matter ω_{cdm} .

Acknowledgements It is a pleasure to thank Steen Hansen, Carolina Odman and Joseph Silk for useful comments. We acknowledge the use of CMB-FAST [40]. AM is supported by PPARC.

-
- [1] E. Torbet *et al.*, *Astrophys. J.* **521** (1999) L79 [arXiv:astro-ph/9905100]; A. D. Miller *et al.*, *Astrophys. J.* **524** (1999) L1 [arXiv:astro-ph/9906421].
- [2] P. D. Mauskopf *et al.* [Boomerang Collaboration], *Astrophys. J.* **536** (2000) L59 [arXiv:astro-ph/9911444]; A. Melchiorri *et al.* [Boomerang Collaboration], *Astrophys. J.* **536** (2000) L63 [arXiv:astro-ph/9911445].
- [3] C. B. Netterfield *et al.* [Boomerang Collaboration], arXiv:astro-ph/0104460.
- [4] N. W. Halverson *et al.*, arXiv:astro-ph/0104489.
- [5] A. T. Lee *et al.*, *Astrophys. J.* **561** (2001) L1 [arXiv:astro-ph/0104459].
- [6] T. J. Pearson *et al.*, arXiv:astro-ph/0205388.
- [7] P. F. Scott *et al.*, arXiv:astro-ph/0205380.
- [8] P. de Bernardis *et al.*, [Boomerang Collaboration], arXiv:astro-ph/0105296.
- [9] C. Pryke, N. W. Halverson, E. M. Leitch, J. Kovac, J. E. Carlstrom, W. L. Holzapfel and M. Dragovan, arXiv:astro-ph/0104490.
- [10] R. Stompor *et al.*, *Astrophys. J.* **561** (2001) L7 [arXiv:astro-ph/0105062].
- [11] X. Wang, M. Tegmark, M. Zaldarriaga, arXiv:astro-ph/0105091.
- [12] J. L. Sievers *et al.*, arXiv:astro-ph/0205387.
- [13] J. A. Rubino-Martin *et al.*, arXiv:astro-ph/0205367.
- [14] A. Lewis and S. Bridle, arXiv:astro-ph/0205436.
- [15] A. Melchiorri and J. Silk, arXiv:astro-ph/0203200.
- [16] C. J. Odman, A. Melchiorri, M. P. Hobson and A. N. Lasenby, arXiv:astro-ph/0207286.
- [17] S. H. Hansen *et al.*, *Phys. Rev. D* **65**, 023511 (2002) [arXiv:astro-ph/0105385].
- [18] W. J. Percival *et al.*, arXiv:astro-ph/0105252.
- [19] SDSS collaboration, arXiv:astro-ph/0107417.
- [20] G. Efstathiou *et al.*, arXiv:astro-ph/0109152.
- [21] O. Lahav *et al.*, arXiv:astro-ph/0112162.
- [22] R. Bean and A. Melchiorri, *Phys. Rev. D* **65** 041302 (2002) [arXiv:astro-ph/0110472].
- [23] W. J. Percival *et al.*, arXiv:astro-ph/0206256.
- [24] S. Hannestad and E. Mortsell, astro-ph/0205096.
- [25] S. Hannestad, astro-ph/0205223.
- [26] O. Elgaroy *et al.*, *Phys. Rev. Lett.* **89** 061301 (2002).
- [27] D. H. Lyth and A. Riotto, *Phys. Rept.* **314** 1 (1999) [arXiv:hep-ph/9807278].
- [28] A. R. Liddle and D. H. Lyth, "Cosmological Inflation And Large-Scale Structure," *Cambridge, UK: Univ. Pr. (2000) 400 p.*
- [29] D. H. Lyth and D. Wands, *Phys. Lett. B* **524**, 5 (2002) [arXiv:hep-ph/0110002]; D. H. Lyth, C. Ungarelli and D. Wands, arXiv:astro-ph/0208055; K. Dimopoulos and D. H. Lyth, arXiv:hep-ph/0209180.
- [30] E. D. Stewart, *Phys. Lett.* **391B**, 34 (1997) [arXiv:hep-ph/9606241].
- [31] E. D. Stewart, *Phys. Rev. D* **56**, 2019 (1997) [arXiv:hep-ph/9703232].
- [32] L. Covi, D. H. Lyth and L. Roszkowski, *Phys. Rev. D* **60**, 023509 (1999) [arXiv:hep-ph/9809310].
- [33] L. Covi and D. H. Lyth *Phys. Rev. D* **59**, 063515 (1999) [arXiv:hep-ph/9809562].
- [34] L. Covi *Phys. Rev. D* **60**, 023513 (1999) [arXiv:hep-ph/9812232].
- [35] G. German, G. Ross and S. Sarkar, *Phys. Lett.* **469B**, 46 (1999) [arXiv: hep-ph/9908380].
- [36] D.H. Lyth and L. Covi, *Phys. Rev. D* **62** 103504 (2000) [arXiv:astro-ph/0002397].
- [37] L. Covi and D. H. Lyth, *MNRAS*, Vol. 326, 885-893 (2001) [arXiv:astro-ph/0008165].
- [38] S. Hannestad, S.H. Hansen and F.L. Villante, *Astropart. Phys.* **16**, 137-144 (2001) [arXiv:astro-ph/0012009]; S. Hannestad, S.H. Hansen, F.L. Villante and A.J.S. Hamilton, *Astropart. Phys.* **17**, 375-382 (2002) [arXiv:astro-ph/0103047].
- [39] L. Randall, M. Soljagic and A. H. Guth, *Nucl. Phys. B* **472**, 377 (1996) [arXiv:hep-ph/9512439].
- [40] U. Seljak and M. Zaldarriaga, *Astrophys. J.* , 469, 437 (1996) [arXiv:astro-ph/9603033].
- [41] N. Gnedin, arXiv:astro-ph/0110290.
- [42] N. Aghanim, P. G. Castro, A. Melchiorri and J. Silk, arXiv:astro-ph/0203112.
- [43] S. L. Bridle, R. Crittenden, A. Melchiorri, M. P. Hobson, R. Kneissl and A. N. Lasenby, arXiv:astro-

- ph/0112114.
- [44] M. Tegmark, A.J.S. Hamilton, Y. Xu, arXiv:astro-ph/0111575.
- [45] R. A. Croft *et al.*, arXiv:astro-ph/0012324.
- [46] N. Dalal and C.S. Kochanek, arXiv:astro-ph/0202290.
- [47] U. Seljak, arXiv:astro-ph/0111362.
- [48] A. Refregier *et al.*, arXiv:astro-ph/0203131.
- [49] C. Caprini, S. H. Hansen and M. Kunz, arXiv:hep-ph/0210095.